KIF4A promotes genomic stability and progression of endometrial cancer through regulation of TPX2 protein degradation

Jun Zhang
Huazhong University of Science and Technology Tongji Medical College
Lanfen An
Huazhong University of Science and Technology Tongji Medical College
Zhicheng Yu
Huazhong University of Science and Technology Tongji Medical College
Rong Zhao
Huazhong University of Science and Technology Tongji Medical College
Rui Shi
Huazhong University of Science and Technology Tongji Medical College
Xing Zhou
Huazhong University of Science and Technology Tongji Medical College
Sitian Wei
Huazhong University of Science and Technology Tongji Medical College
Qi Zhang
Huazhong University of Science and Technology Tongji Medical College
Tangansu Zhang
Huazhong University of Science and Technology Tongji Medical College
Dilu Feng
Huazhong University of Science and Technology Tongji Medical College
Shuaijun Chen
Huazhong University of Science and Technology Tongji Medical College
Hongbo Wang (hb_wang1969@sina.com)
Huazhong University of Science and Technology Tongji Medical College https://orcid.org/0000-0001-7090-1750

Research Article

Keywords: Endometrial cancer, kinesin, KIF4A, TPX2, DNA damage response

Posted Date: May 9th, 2022

DOI: https://doi.org/10.21203/rs.3.rs-1601949/v1

Abstract

Background

Kinesin family member 4A (KIF4A) belongs to the kinesin superfamily proteins, which are closely associated with mitophagy. However, the role of KIF4A in endometrial cancer (EC) remains poorly characterized. Here, we aimed to explore the function and regulatory mechanisms of KIF4A in EC.

Methods

The expression of KIF4A was evaluated by quantitative polymerase chain reaction, western blotting, and immunohistochemistry. Cell proliferation was measured using Cell Counting Kit-8, clone formation, and 5-ethynyl-2'-deoxyuridine staining assays. Flow cytometry was performed using annexin V/propidium iodide (PI) to identify apoptotic cells and PI staining to analyze the cell cycle. RNA-seq, coimmunoprecipitation, immunofluorescence, and western blotting were performed to explore the underlying mechanism.

Results

In this study, we demonstrated that KIF4A was upregulated and predicted a poor prognosis in patients with EC. KIF4A knockdown in EC cells resulted in attenuated proliferative capacity and promoted cell cycle arrest and apoptosis induced by increased DNA damage. Mechanistic investigations indicated that KIF4A knockdown exacerbated DNA damage repair and response by regulating the stability of the spindle assembly factor TPX2.

Conclusions

KIF4A promotes genomic stability and progression of endometrial cancer through regulation of TPX2 protein degradation. KIF4A may serve as a promising therapeutic target for endometrial cancer

Background

Endometrial cancer (EC) is one of the most common gynecological tumors worldwide, and its incidence is increasing[1, 2]. EC is generally classified into two types according to whether the tumor is sensitive to estrogen. Type 1 EC is estrogen dependent and represents 75–90% of EC, whereas type 2 is estrogen independent[3]. Currently, the treatment of EC remains mainly surgical, including total hysterectomy, salpingo-oophorectomy, and pelvic lymph node dissection[4, 5]. Patients with EC in the early stage (stage I or II) have a relatively favorable prognosis, with 5-year overall survival rates of 95% and 69% for stages I and II, respectively. However, for patients with advanced stage (stage III or IV), the prognosis is poor, and the 5-year survival rate is only 15–17%[5–7]. Therefore, there is an urgent clinical need to elucidate the

molecular mechanism of EC progression and identify novel diagnostic markers and therapeutic targets for patients with EC.

Kinesins are microtubule-based motor proteins that mediate diverse functions within the cell, including the transport of vesicles, organelles, chromosomes, and protein complexes and the movement of microtubules[8, 9]. Individual kinesin family members have specific functions. Some kinesins are involved in axonal transport, whereas others function exclusively during mitosis[10]. To date, 45 kinesin superfamily proteins (KIFs) with varying functions have been discovered in humans[11], and at least 12 of them are required in various aspects of mitosis, including bipolar spindle assembly, chromosome alignment, chromosome segregation, and cytokinesis[12, 13]. Multiple kinesins also promote the proliferation and progression of pancreatic cancer[14], hepatocellular carcinoma [15–17], glioblastoma[18, 19], melanoma[20, 21], and lung adenocarcinoma[22]. KIFC1 and KIF2C are upregulated and accelerate the proliferation of EC[23, 24]. However, the role of kinesins in EC has not yet been fully investigated.

In the present study, to evaluate the role of kinesins in EC, we analyzed differentially expressed kinesins in The Cancer Genome Atlas-Uterine Corpus Endometrial Carcinoma (TCGA-UCEC) and GSE17025 databases and found that kinesin family member 4A (KIF4A) was most prominently upregulated. Furthermore, we demonstrated that KIF4A accelerated EC progression by regulating cell proliferation and division by inhibiting the apoptosis of EC cells. Mechanistic investigations demonstrated that KIF4A promotes tumor growth by regulating the stability of TPX2 and enhances resistance to endogenous DNA damage induced by replication stress. Taken together, these results establish that KIF4A/TPX2 facilitates EC progression by regulating the DNA damage response (DDR) during the mitosis of tumor cells.

Methods

Cell Culture and transfection.

Human endometrial cancer cell lines KLE (RRID:CVCL_1329), Ishikawa (RRID:CVCL_2529), HEC-1-A (RRID:CVCL_0293), HEC-1-B (RRID:CVCL_0294), and RL95-2 (RRID:CVCL_0505) were obtained from the American Type Culture Collection (ATCC). KLE, RL95-2, and Ishikawa were maintained in DMEM/F12 medium containing 10% fetal bovine serum (FBS) (Gibco); HEC-1-A was maintained in McCoy's 5A medium containing 10% FBS. HEC-1-B was maintained in MEM medium containing 10% FBS. Cells were cultured in a 5% CO_2 incubator at 37 °C. All the cell lines have been fully authenticated using STR profiling within the last 3 years and tested free of mycoplasma.

The small hairpin RNA (shRNA) of KIF4A was synthesized and cloned into the LV3-shRNA vector by GenePharma (Shanghai, China); the shRNA sequences are listed in Supplementary Table S1. KLE and Ishikawa cells with KIF4A shRNA knockdown were generated using a lentiviral–mediated delivery system at a multiplicity of infection (MOI) of 30 using Polybrene. Cells were selected using 2 μg/mL puromycin for 48 h to establish stable cell lines. Human TPX2 (NM_012112) cDNA was amplified with PCR and

cloned into an SV40 lentiviral vector (GeneChem, Shanghai, China). For plasmid transfections, KLE and Ishikawa cells were cultured in six-well plants and transfected with 5 μg expression plasmids for TPX2

or control vector using Lipofectamine 3000 (Invitrogen, CA, USA) according to the manufacturer's instructions. Protein lysates and total RNA were collected 72 h after the transfection to verify transfection efficiency by western blot and qPCR.

Protein synthesis inhibitor cycloheximide (CHX), proteasome inhibitor MG132, and autophagy inhibitor chloroquine were all purchased from Selleck (Houston, TX, USA), and these were diluted in dimethyl sulfoxide (DMSO) solvent to obtain a stock concentration.

Databases and clinical information

The mRNA levels of patients with UCEC and corresponding clinical information were obtained from the TCGA (https://portal.gdc.cancer.gov/) and GEO databases (https://www.ncbi.nlm.nih.gov/geo/). The R packages "edgeR" and "limma" were used for normalization and differential gene expression analysis with the R statistical software (version 4.1.0). The criteria for screening differentially expressed genes were as follows: FDR $p < 0.05$ and $|\log \text{fold change}| > 2$. The gene set enrichment analysis (GSEA) in UCEC with the high and low expression levels of KIF4A was conducted by comparing with the reference c2 gene sets (KEGG gene sets and Reactome gene sets) from the Molecular Signatures Database using GSEA v.4.0.2 (http://software.broadinstitute.org/gsea/msigdb/index.jsp). The number of permutations was set at 1,000. Values of $|NES| > 1$, $p < 0.05$, and FDR < 0.25 were considered statistically significant.

Patient samples.

Human EC tissues and adjacent normal tissues were all obtained from patients who underwent surgery in the Department of Obstetrics and Gynecology of Wuhan Union Hospital (Tongji Medical College, Huazhong University of Science and Technology). All samples were stored in liquid nitrogen at −80 °C until use. None of the patients had received preoperative radiotherapy, hormonal treatment, or chemotherapy. The patients provided informed consent for this process of the study. Our study protocols were approved by the Institutional Review Board of Huazhong University of Science and Technology.

Western blot analysis.

Protein expression levels were measured using western blot. The cells or tissues were lysed in ice-cold lysis buffer containing a protease inhibitor cocktail (Selleck, Shanghai, China). Isolated protein was quantified using the Pierce BCA protein kit (23225, Thermo, Waltham, USA) according to the manufacturer's instructions. Western blot was performed according to the standard protocol. Briefly, these protein samples were loaded on 6-12.5% SDS-PAGE gels. Following blotting, the blots were blocked with 5% BSA (Servicebio, Wuhan, China) for 1 h at room temperature and incubated with appropriate primary

antibodies at 4°C overnight. The blots were incubated with appropriate HRP conjugated secondary antibodies (ABclonal, Wuhan, China) at room temperature for 1 h. Development of membranes was performed with enhanced chemiluminescence (Biosharp, Beijing, China) and the intensity was measured using a ChemiDoc XRS with Image Lab Software (Bio-Rad, CA, USA). The antibodies used are listed in Supplementary Table S2.

RNA extraction and qRT-PCR.

For gene expression studies, the total RNA from cells and tissues was isolated with TRIZOL® reagents (Takara, Otsu, Japan). RNA extraction was performed according to the manufacturer's protocols. RNA was reverse transcribed into cDNA by RT-PCR using Hiscript@ QRT SuperMix (Vazyme, Nanjing, China) in a 20 μl total sample volume. The parameters of reaction were as follows: 95°C for 30 s, followed by 40 cycles at 95°C for 5 s and 60°C for 1 min. Next, the genes expression levels were measured by quantitative PCR (qPCR). qPCR was performed in a CFX Connect Real-Time PCR Detection System (Bio-Rad, Hercules, CA, USA) using SYBR green supermix (Vazyme, Nanjing, China). The total amount of mRNA was normalized to endogenous GAPDH mRNA. The $2^{-\Delta\Delta Ct}$ method was used to calculate the related genes expression levels. The primer sequences are listed in Supplementary Table S3.

Immunohistochemistry and immunofluorescence staining

Paraformaldehyde-fixed, paraffin-embedded tumors or normal tissues were mounted on glass slides in 4-μm thick sections, and slides were dewaxed, dehydrated, and rehydrated successively. Then, the slides were incubated with appropriate primary antibodies at 4°C overnight, followed by incubation with the horseradish peroxidase-conjugated immunoglobulin (Ig)G secondary antibody at room temperature for an hour (Abclonal, Wuhan, China). All the slides were observed by light microscopy connected with a digital camera. Immunohistochemistry score (IHC score) was determined by two independent, blinded investigators. IHC score = staining intensity * staining area. There are four levels of staining intensity: negative = 0; weak = 1; moderate = 2; and strong = 3. Area of staining was quantified using ImageJ, as follows: <10% positive cells = 0, 10–25% = 1, 25–50% = 2, 50–75% = 3, and 75–100% = 4.

For immunofluorescent staining, cells (3 × 104) were fixed in 4% paraformaldehyde at 24 h after seeding. Cells were permeabilized with 0.5% TritonX-100 for 10 min and blocked with 5% goat serum. Next, the cells were incubated with primary antibodies (γH2AX, Abmart, TA3187, 1:100). Finally, FITC-conjugated AffiniPure Goat Anti-rabbit IgG (H+L) (BOSTER, BA1105, 1:200) was used as the secondary antibody. 4',6-diamidino-2-phenylindole (DAPI) (Beyotime, Shanghai, China) was used to stain the nuclei.

Animal model and treatments.

Female 4-week-old BALB/c-nu nude mice were purchased from VitalRiver (Beijing, China). Stably transfected KLE cells were washed by serum-free medium twice and injected subcutaneously into nude

mice (5×10^6 cells/site). A digital caliper was used to access the tumor growth every four days for 4 weeks. Mice were euthanized on day 32 after cell implantation. The subcutaneous xenograft model experiment was approved by the Animal Care and Use Committee of Tongji Medical College of Huazhong University of Science and Technology.

Co-immunoprecipitation (CO-IP) assay

Co-IP experiments were performed according to the manufacturer's instructions. Cultured cells were lysed using ice-cold non-denaturing lysis buffer with protease inhibitor cocktail. After cell lysis at 4°C for 1 h and protein lysate separation, the whole cell lysate was incubated with the appropriate antibody at 4°C overnight. Then the Ab-Ag complex was added with Protein A/G Magnetic Beads (MCE, Shanghai, China) and rotated for 2 h at 4°C to allow the Ab-Ag complex to bind to the Protein A/G Magnetic Beads. The protein A/G Magnetic Beads-Ab-Ag complex was boiled in 2X SDS loading buffer and transferred the bead suspension into a clean tube. SDS-PAGE and Western blotting analysis were used to detect cross-correlations of the related protein in whole-cell lysate.

Cell proliferation assays

The proliferation of cells was analyzed with the colony formation assays; 1000 cells were plated into six-well plates to evaluate the effects of colony formation. Two weeks after cell seeding, surviving colonies (>50 cells per colony) were visualized with 0.05% crystal violet staining. KLE and Ishikawa cells were seeded into 96-well plates (2000 cells per well). After incubation for 0, 24, 48, 72, and 96 h, the medium was added with 100 μl of complete medium containing 10 μl of CCK-8 reagent (Topscience, Shanghai, China) for 1h at 37 °C. The absorbances were subsequently measured at 450 nm. An EdU assay was conducted utilizing an EdU immunofluorescence staining kit (Beyotime, Shanghai, China).

Cell-cycle analysis

Cell cycle progression was detected by flow cytometry and was performed as per the manufacturer's protocols. After treatment, cells were collected and centrifuged at 1000 rpm for 5 min. Then, the cells were fixated in 70% to 80% ethanol at 4°C for 24 h. After washing the cells twice to remove ethanol, they were resuspended in 0.5 ml PI/RNase staining buffer (BD, San Jose, CA, USA) and incubated for 15 min at room temperature. The distribution of cell cycle phases was determined by a BD LSRFortessa (BD, San Jose, CA, USA) and analyzed using ModFit software.

Apoptosis analysis

Analysis of apoptosis was performed using FITC Annexin V Apoptosis Detection Kit I (BD Biosciences, NJ, USA). Briefly, cells were seeded and cultured for 48 h. After washing the cells with 4°C phosphate

buffered saline (PBS), they were stained with Annexin V-FITC/PI for 20 min in dark at room temperature and then analyzed immediately. The stained cells were detected using the BD LSRFortessa machine and analyzed with the FlowJo version 7 software module.

RNA Sequencing and Analysis.

RNA-Seq was performed by CapitalBio Technology on an Illumina NovaSeq sequencer (Illumina). The total RNA of KLE cells with or without KIF4A knockdown were isolated using TRIzol reagent, according to the manufacturer's protocol. The sequencing data were filtered by FastQC (v0.11.5) and NGSQC (v2.3.3) to remove the low-quality data. Gene expression analyses were conducted with StringTie (v1.3.3b). Differentially expressed genes were identified using the "DESeq" R package. The screening criteria for the DEGs were as follows: $|\log FC| \geq 2$ and $P<0.05$. The annotation of the DEGs was carried out based on the information obtained from the databases of Ensemble, National Center for Biotechnology Information (NCBI), Uniprot, GO, and Kyoto Encyclopedia of Genes and Genome (KEGG).

Statistical analysis

All the experiments were performed in triplicate and statistical analysis was performed using GraphPad 7.0. The Kaplan-Meier (KM) method was also used for survival analysis, and log-rank tests were applied to evaluate differences between groups. Values are expressed as the mean ± SEM. Statistical analyses were conducted using the one-way analysis of variance (one-way ANOVA) and Student's t-test. *P* values < 0.05 were considered statistically significant.

Results

Kinesin family member 4A (KIF4A) is highly expressed in endometrial cancer (EC)

Kinesins have been found to be dysregulated in a variety of tumors. To explore the expression levels of KIFs in uterine corpus endometrial carcinoma (UCEC) and normal endometrial tissues, TCGA database and Gene Expression Omnibus data were analyzed. We found 11 common upregulated KIFs (KIF1A, KIF2C, KIF4A, KIF11, KIF14, KIF15, KIF18A, KIF18B, KIF20A, KIF23, and KIFC1) and one common downregulated KIF (KIF26A) in TCGA-UCEC and GSE17025 databases (Fig. S1A, B). By detecting the mRNA level of kinesin in EC tissue samples, we found that KIF4A increased most significantly in EC (fold change = 3.64, $P < 0.01$) (Fig. 1A). Furthermore, in TCGA and GSE17025 databases, the mRNA expression of KIF4A was significantly upregulated in EC tissues (Fig. 1B, C). We also selected 23 paired samples from TCGA database and performed a paired t-test on the expression level of KIF4A, which was consistent with the overall results (Fig. 1D). Interestingly, we observed that KIF4A was elevated in all cancer types, compared to that in normal tissues (Fig. 1E). Regarding protein levels, western blot results showed that KIF4A was increased in human EC compared to adjacent normal tissues. In addition,

immunohistochemical staining for KIF4A was performed in paraffin sections obtained from 20 normal and 35 tumor tissue samples, which suggested that KIF4A was highly expressed in EC tissues (Fig. 1G).

KIF4A acts as an indicator of unfavorable outcomes in patients with EC

We further explored the prognostic value of KIF4A in patients with UCEC by combining clinical data from the TCGA database. The patients were divided into two groups (high vs. low) based on the median expression of KIF4A across all samples. Overall survival (OS), disease-free interval (DFI), disease-specific survival (DSS), and progression-free interval (PFI) were estimated using the Kaplan–Meier method, and the results indicated that the high expression of KIF4A led to statistically significant inferior outcomes compared with that of the low KIF4A expression group (OS: HR, 1.750, 95% confidence interval (CI)= 1.153–2.658; PFI: HR, 2.026 ,95% CI = 1.417–2.897; DSS: HR, 1.978 ,95% CI = 1.183–3.305; DFI: HR, 1.925 ,95% CI = 1.137–3.259) (Fig. 2A–D). Next, we analyzed the correlation between KIF4A expression and the clinicopathological features of the patients (Table 1). The expression level of KIF4A was highly correlated with the pathological type, clinical stage, histologic grade, age, and vital status in patients with EC (Fig. 2E–I). Receiver operating characteristic curves were used to analyze the diagnostic value of KIF4A in TCGA-UCEC and GSE17025 databases. As shown in Fig. 2J–L, KIF4A had a high area under the curve value in patients with EC, indicating that KIF4A could effectively distinguish EC tissues from normal tissues. Collectively, these results indicate that KIF4A is upregulated and predicts poor prognosis in EC.

KIF4A promotes EC cell proliferation

We next determined KIF4A protein expression levels in normal human endometrial cells and several human EC cell lines by western blotting and quantitative polymerase chain reaction. Subsequent analyses were restricted to the KLE and Ishikawa cell lines because of their heightened KIF4A expression (Fig. 3A, B). Therefore, to elucidate the function of KIF4A in cell proliferation, we designed three independent shRNAs to knock down KIF4A expression in KLE and Ishikawa cells. KIF4A silencing was verified by quantitative real-time polymerase chain reaction (qRT-PCR) and western blotting (Fig. 3C, D). Colony formation, Cell Counting Kit-8 (CCK-8), and 5-ethynyl-2'-deoxyuridine (EdU) assays were used to measure the effect of KLE and Ishikawa cell proliferation and growth, which indicated that the cell growth and colony formation potential were significantly reduced in EC cells with stable expression of KIF4A shRNA (Fig. 3E–G).

Knockdown of KIF4A leads to cell cycle arrest and apoptosis

To further clarify the role of KIF4A in cell proliferation regulation, we performed gene set enrichment analysis (GSEA) of the TCGA-UCEC database, which revealed that the top signatures in the high KIF4A group were strongly associated with cell cycle andapoptosis (Fig. S2A–C). Thus, we hypothesized that

KIF4A may be involved in regulating cell cycle progression. Flow cytometry was performed to evaluate its effect on the cell cycle status. As hypothesized, KIF4A knockdown increased the proportion of cells in the G2/M phase and decreased that in the S phase (Fig. 4A). Western blot results verified that the protein levels of the G2/M phase marker, cyclin B1, and CDK1 also decreased in EC cells with KIF4A knockdown (Fig. 4B). Next, the effect of KIF4A on EC cell apoptosis was measured by flow cytometry apoptosis assay, which demonstrated that KIF4A knockdown significantly increased the apoptosis rate (Fig. 4C). Similarly, KIF4A knockdown upregulated the expression of Bax, cleaved caspase 3, and decreased the expression of Bcl-2 (Fig. 4D). These results suggest that KIF4A knockdown induces G2/M phase arrest and promotes apoptosis of EC cells.

KIF4A knockdown activates DNA damage response signaling

To explore the downstream functional roles of KIF4A, RNA sequencing was performed in KLE cells stably knocked down KIF4A (sh-KIF4A vs. sh-Control). A total of 1621 differentially expressed genes (DEGs) were identified in cells stably knocked down KIF4A compared with sh-Control, with 1286 genes upregulated and 335 downregulated(Fig. 5A, B). To further analyze the DEGs, pathway enrichment analysis was performed, and the results revealed that mitotic G2-G2/M phases, cell cycle checkpoints, apoptosis, nucleotide excision repair, and DNA double-strand break repair pathways were activated simultaneously (Fig. 5C). Subsequently, Gene Ontology enrichment analysis indicated that these genes were predominantly enriched in cell cycle, DNA repair, apoptotic signaling pathway, G2/M transition of mitotic cell cycle, double-strand break repair, and ubiquitin (Ub)-dependent protein catabolic process (Fig. 5D). Furthermore, GSEA indicated that KIF4A was also highly associated with homology-directed repair, chromosome maintenance, DNA double-strand break response, G2/M DNA damage checkpoint, and Hub-specific processing protease pathway in the TCGA-UCEC database (Fig. S2D–I). These results suggest that KIF4A may be involved in DDR signaling.

DDR is composed of a coordinated network of signaling pathways that sense DNA damage and induce cellular responses through a set of DNA repair mechanisms. Double-strand breaks (DSBs) are the most deleterious DNA damage that leads to chromosomal aberrations, genomic instability, or cell death. Phosphorylation of H2AX (γH2AX) plays a key role in DDR as γH2AX is necessary for the DNA repair process, and γH2AX activates checkpoint proteins that arrest cell cycle progression[25]. Histone H2AX is a substrate of several phosphoinositide 3-kinase-related protein kinases, such as ataxia-telangiectasia mutated (ATM), Rad3-related kinase, and DNA-dependent protein kinase[26]. DDR signaling was assessed by examining the phosphorylation status of key DDR signaling molecules, including histone H2AX (γH2AX), ATM, and CHK2[27]. During mitosis of eukaryotic cells, the separation of sister chromosomes is mainly mediated by kinesins, which bind to chromosomes, move along microtubules, and exert tension and thrust on centrosomes[28]. Therefore, kinesins are important for the maintenance of genomic stability. Previous studies have also shown that KIF2C depletion or inhibition leads to the accumulation of endogenous DNA damage[29]. KIF18B and KIFC1 have been reported to promote 53BP1-mediated DNA double-strand break repair[30] .

Therefore, to further elucidate the pathway that mediated cell apoptosis, we examined

the effect of KIF4A knockdown on phosphorylation of H2AX, ATM, and CHK2. Western blotting showed that KIF4A knockdown EC cells had increased DDR pathway activity, as evidenced by elevated pATM, pCHK2, and γH2AX levels. Furthermore, immunofluorescence staining was performed using an anti-γH2AX antibody, which suggested that EC cells with stable KIF4A knockdown could form more numerous DNA-damage-induced nuclear foci. Collectively, these results indicate that KIF4A knockdown causes DNA damage accumulation and upregulates cellular DDR-related gene expression.

KIF4A regulates the protein stability of TPX2

To identify the association between KIF4A and DDR signaling pathways in EC cells, we utilized a system-level approach to understand functional protein interactions (http://string-db.org/), and the top 10 KIF4A-interacting proteins were identified (Fig. 6A). We then set out to confirm whether an interaction exists between KIF4A and these 10 proteins. We used western blotting to examine the protein levels of these proteins in Ishikawa and KLE cells with KIF4A knockdown. Notably, CDK1 and TPX2 expressions were significantly downregulated in EC cells after KIF4A knockdown compared to that in control cells (Fig. 6B, Fig. S3A). Moreover, the qRT-PCR results showed that KIF4A knockdown repressed CDK1 mRNA levels but had no effect on TPX2 mRNA levels (Fig. 6C, Fig. S3B). The inconsistency between the protein and mRNA levels of TPX2 suggests that KIF4A may regulate TPX2 levels by regulating the stability of TPX2 protein.

To further verify whether KIF4A interacts with TPX2, coimmunoprecipitation was performed, and the results revealed that endogenous KIF4A could bind to TPX2 in EC cells (Fig. 6D, E). Subsequently, KLE and Ishikawa cells with stable knockdown of KIF4A were treated with cycloheximide (CHX) to inhibit protein synthesis, and TPX2 protein turnover was analyzed over time. Compared with that in the control cells, the TPX2 half-life was considerably decreased in EC cells with stable knockdown of KIF4A, which were treated with CHX (Fig. 6F). The Ub-proteasome and autophagy-lysosome pathways are the two main routes of protein degradation in eukaryotes[31]. To determine which pathway played a major role in this process, a proteasome inhibitor (MG132) and a lysosome inhibitor (chloroquine) were administered to KIF4A knockdown cells. Strikingly, only MG132 completely restored the TPX2 protein level in KIF4A knockdown EC cells compared to that in the untreated control (Fig. 6G).

Our data suggest that knockdown of KIF4A represses TPX2 protein stability mainly by promoting protein degradation mediated by the Ub/proteasomal pathway. Next, we analyzed the effect of KIF4A knockdown on the ubiquitination of endogenous TPX2 through both immunoprecipitation and western blotting, which showed that the level of ubiquitinated TPX2 was significantly higher in EC cells with the stable knockout of KIF4A compared to control cells (Fig. 6H). In general, the above results indicate that KIF4A regulates TPX2 protein stability by affecting TPX2 ubiquitination levels.

TPX2 is required for KIF4A-mediated tumor progression

TPX2 is a multifunctional protein that includes one or more potential microtubule-binding sites that play a vital role in spindle assembly[32]. Other recent studies also reported that TPX2/Aurora A could protect DNA forks during replication stress[33].

To further verify whether KIF4A induced EC progression by regulating the levels of TPX2, rescue experiments were performed. We co-transfected sh-KIF4A and pcDNA-TPX2 into KLE and Ishikawa cells. Next, we examined the effect of TPX2 overexpression on KIF4A knockdown-induced suppression of proliferation in vitro. The CCK-8 assay indicated that TPX2 overexpression could reverse the KIF4A knockdown-induced inhibition of proliferation (Fig. 7A, B). The EdU assay showed that TPX2 overexpression could rescue the decrease in EdU-positive cells induced by KIF4A knockdown (Fig. 7C). Moreover, we examined the influence of TPX2 overexpression on KIF4A knockdown-induced cell cycle arrest and apoptosis, which indicated that TPX2 overexpression impairs the KIF4A knockdown-mediated increase in EC cell cycle arrest and apoptosis (Fig. S3C). Furthermore, immunofluorescence staining of γH2AX also revealed that TPX2 overexpression markedly reduced the number of γH2AX foci (Fig. 7D). Meanwhile, a western blot was performed to probe the effect of TPX2 overexpression on the DDR signaling pathway, which suggested that TPX2 overexpression could suppress the expression of pATM, pCHK2, and γH2AX induced by KIF4A knockdown (Fig. 7E). Based on the above observations, we concluded that KIF4A mediated tumor promotion through TPX2-dependent signaling.

A subcutaneous xenograft tumor model is used to confirm the role of KIF4A in EC

Based on the observations described above, we examined the effects of KIF4A on EC cell proliferation in vivo by stably transfecting KLE cells with sh-KIF4A or sh-NC and subcutaneously injecting into nude mice (n = 5 per group). Tumor volume was measured every 4days after injection. After 32 days, the mice were euthanized, and whole tumors were excised. The results demonstrated that KIF4A knockdown significantly reduced both the weight and volume of tumors in vivo (Fig. 8A–C). Immunohistochemical staining was performed to evaluate the expressions of KIF4A and TPX2 in xenograft tumors, and the results were consistent with the in vitro findings. The decrease in KIF4A expression was accompanied by decreased levels of TPX2 (Fig. 8D). The expression of ki-67, a proliferation marker, was also decreased in sh-KIF4A EC tumors. Collectively, these results suggest that KIF4A functions as a tumor promoter in EC and that KIF4A promotes EC cell progression via TPX2.

Discussion

EC is more likely to be diagnosed at an early stage, with a good overall survival[34]. However, advanced EC has a poor prognosis; the continued annual increase in morbidity and mortality of EC underscores a dire need for more efficient approaches for this malignancy[35]. Various kinesin genes have been reported to be upregulated in several cancers and promote tumor proliferation and progression; however, the role of kinesins in EC has not been fully elucidated.

KIF4A is a kinesin-4 family member, which is highly expressed in a variety of tumors and promotes the progression of cancers[9, 36–40]. In this study, we demonstrated that KIF4A is highly elevated in EC tissues compared to normal tissues. Moreover, high levels of KIF4A expression were significantly correlated with several clinicopathological features, such as Federation Internationale de Gynecologie et d'Obstetrique stage, pathology type, clinical stage, histologic grade, and age. In addition, high KIF4A expression was associated with poorer OS, PFI, DSS, and DFI in patients with EC. These findings revealed that KIF4A plays a significant role in the progression of EC and can act as a potential therapeutic target and clinical biomarker for patients with EC.

DNA damage is a key factor in both the evolution and treatment of cancer, which gives rise to an abnormal nucleotide or nucleotide fragment, causing a break in one or both chains of the DNA strand. When DNA is damaged, the possibility of generated mutations increases[41]. Genomic instability is one of the most important factors that lead to cancer development, and genomic instability is a common feature of cancer cells, which favors the accrual of driver mutations and the expansion of tumor heterogeneity[42, 43]. The DDR pathways contain a class of proteins that detect DNA DSBs, chromosomal fragmentation, translocation, and deletions and can correct some alterations, which protect cancer cells from death due to endogenous and external DNA damage factors[44]. Anticancer radiotherapies or chemotherapies generally eliminate tumor cells by damaging DNA, inducing apoptosis, and blocking tumor cell progression. However, cancer cells usually acquire resistance to cancer therapy, which is associated with common DNA repair mechanisms. Thus, targeting the DDR pathway is a promising therapeutic strategy for cancer treatment. Several drugs that target proteins involved in various DNA repair processes have been developed, such as poly ADP ribose polymerase 1 (PARP1) inhibitors, which induce synthetic lethality in tumor cells deficient in homologous recombination[45]. PARP1 inhibitors have been extensively investigated for the treatment of various cancer types[46]. However, as HR-deficient tumors represent only a small fraction of ECs, the therapeutic utility of PARP inhibitors is limited in this disease[47]. Previous studies have shown that KIF4A has vital functions in mitosis, including chromosome condensation, spindle organization, chromosome segregation, and cytokinesis[48, 49]. KIF4A has been found to be associated with BRCA2, which is required for Rad51 recruitment to sites of DNA damage in the HR pathway. KIF4A depletion could inhibit ionizing radiation-induced recruitment of Rad51, thereby impairing HR in DNA repair[50]. In addition, Wan et al. found that KIF4A inhibition could aggravate DNA damage and limit the further increase in PARP1 activity induced by cisplatin in human non-small cell lung cancer cells[51]. These results indicate that KIF4A overexpression promotes the progression of cancer cells by regulating the DDR pathways. In this study, RNA sequencing and in vitro experiments demonstrated that KIF4A knockdown suppresses cell proliferation by regulating the DDR pathway, inducing TPX2 degradation, thereby promoting DNA damage accumulation, cycle arrest, and apoptosis in EC cells. TPX2 is a spindle assembly factor required for the normal assembly of mitotic spindles, and TPX2 is frequently reported to be significantly increased in various cancers[52–54]. Elevated TPX2 expression positively correlates with tumor grade, stage, lymph node metastasis, recurrence, and poor patient survival[53, 55]. The TPX2/Aurora A kinase heterodimer complex orchestrates mitotic spindle events to maintain genome integrity. Moreover, it counteracts 53BP1

chromatin accumulation to ensure genome stability[56]. Furthermore, Byrum et al. observed that TPX2/Aurora A promotes BRCA1 localization to breaks and that depletion of either TPX2 or Aurora A causes deprotection of stalled replication forks upon replication stress induction[33].

Our study showed that KIF4A regulates the protein stability of TPX2 via the Ub-proteasome pathway. The ubiquitination process is a post-translational modification that is crucial for maintaining protein homeostasis[57]. Normally, ubiquitination is a significantly dynamic process and is counterbalanced by deubiquitinating (DUB) enzymes[58]. Remarkably, several E3 Ub ligases and DUBs, including FBXW7[59], RNF8, RNF168[60], HDAC6[61], HUWE1[62], USP3[63], BAP1[64], USP26, and USP37[65] have been involved in the ubiquitination and deubiquitination of DDR proteins. Each of these E3 ubiquitin ligases or DUBs can influence various aspects of Ub-dependent protein assembly at DSB sites and regulate DDR signaling[66, 67].

Conclusions

In conclusion, this is the first study to explore the role of KIF4A in mediating DDR signaling in EC. We found that KIF4A promotes cell proliferation, knockdown of KIF4A induces cycle arrest and apoptosis, and KIF4A is vital for genomic integrity through the regulation of mitosis and DDR signaling. Mechanistically, KIF4A maintains genome stability by reducing TPX2 ubiquitination, which can inhibit protein degradation and increase the stability of the TPX2 protein. Therefore, targeting the KIF4A/TPX2 axis may provide new concepts and strategies for the treatment of patients with EC.

Abbreviations

EC
Endometrial cancer
KIF4A
Kinesin family member 4A
TCGA
The Cancer Genome Atlas
DDR
DNA damage response
PARP1
poly ADP ribose polymerase 1
FBS
fetal bovine serum
CCK-8
Cell Counting Kit-8 Assay
EdU
5-Ethynyl-2'-deoxyuridine
CHX

cycloheximide
GSEA
gene set enrichment analysis
DAPI
4',6-diamidino-2-phenylindole
OS
Overall survival
DFI
disease-free interval
DSS
disease-specific survival
PFI
progression-free interval
DEGs
differentially expressed genes.

Declarations

Authors' contributions

J.Z. and L.A. contributed equally to this work. J.Z. and H.W. conceived and designed the experiments; L.A., Z.Y, R.Z., R.S., X.Z., S.W., Q.Z., T.Z., Z.W., and D.F. obtained the data and performed preliminary analyses; J.Z., S.C., and H.W. wrote and revised the manuscript, and all authors read and approved the final version of the manuscript.

Acknowledgements

We thank Long Yu for his help with flow cytometry.

Funding

This work was supported by grants from the Fundamental Research Funds for the Central Universities (2019kfyXKJC072), Major Technical Innovation Project in Hubei Province of China (2019ACA138), the National Key Research and Development Program of China (SQ2018YFC010140), and the National Natural Science Foundation of China (81974409).

Ethics approval and consent to participate

This study was approved by the Institutional Review Board of Huazhong University of Science and Technology.

Consent for publication

Not applicable.

Competing interests

The authors declare no conflicts of interest.

References

1. Morice P, Leary A, Creutzberg C, Abu-Rustum N, Darai E. Endometrial cancer. The Lancet. 2016;387:1094–108.
2. Amant F, Mirza MR, Koskas M, Creutzberg CL. Cancer of the corpus uteri. Int J Gynaecol Obstet. 2018;143(Suppl 2):37–50.
3. Bokhman JV. Two pathogenetic types of endometrial carcinoma. Gynecol Oncol. 1983;15:10–7.
4. Lee YC, Lheureux S, Oza AM. Treatment strategies for endometrial cancer: current practice and perspective. Curr Opin Obstet Gynecol. 2017;29:47–58.
5. Urick ME, Bell DW. Clinical actionability of molecular targets in endometrial cancer. Nat Rev Cancer. 2019;19:510–21.
6. de Boer SM, Powell ME, Mileshkin L, Katsaros D, Bessette P, Haie-Meder C, Ottevanger PB, Ledermann JA, Khaw P, Colombo A, et al. Adjuvant chemoradiotherapy versus radiotherapy alone for women with high-risk endometrial cancer (PORTEC-3): final results of an international, open-label, multicentre, randomised, phase 3 trial. Lancet Oncol. 2018;19:295–309.
7. Giannone G, Attademo L, Scotto G, Genta S, Ghisoni E, Tuninetti V, Aglietta M, Pignata S, Valabrega G: **Endometrial Cancer Stem Cells**: **Role**, **Characterization and Therapeutic Implications**. *Cancers (Basel)* 2019, **11**.
8. Miki H, Setou M, Kaneshiro K, Hirokawa N. All kinesin superfamily protein, KIF, genes in mouse and human. Proc Natl Acad Sci U S A. 2001;98:7004–11.
9. Miki H, Okada Y, Hirokawa N. Analysis of the kinesin superfamily: insights into structure and function. Trends Cell Biol. 2005;15:467–76.
10. Ali I, Yang WC. The functions of kinesin and kinesin-related proteins in eukaryotes. Cell Adh Migr. 2020;14:139–52.
11. Lawrence CJ, Dawe RK, Christie KR, Cleveland DW, Dawson SC, Endow SA, Goldstein LS, Goodson HV, Hirokawa N, Howard J, et al. A standardized kinesin nomenclature. J Cell Biol. 2004;167:19–22.
12. Zhu C, Zhao J, Bibikova M, Leverson JD, Bossy-Wetzel E, Fan JB, Abraham RT, Jiang W. Functional analysis of human microtubule-based motor proteins, the kinesins and dyneins, in mitosis/cytokinesis using RNA interference. Mol Biol Cell. 2005;16:3187–99.

13. Huszar D, Theoclitou ME, Skolnik J, Herbst R. Kinesin motor proteins as targets for cancer therapy. Cancer Metastasis Rev. 2009;28:197–208.
14. Liu ZH, Dong SX, Jia JH, Zhang ZL, Zhen ZG. KIF3B Promotes the Proliferation of Pancreatic Cancer. Cancer Biother Radiopharm. 2019;34:355–61.
15. Chen J, Li S, Zhou S, Cao S, Lou Y, Shen H, Yin J, Li G. Kinesin superfamily protein expression and its association with progression and prognosis in hepatocellular carcinoma. J Cancer Res Ther. 2017;13:651–9.
16. Han J, Wang F, Lan Y, Wang J, Nie C, Liang Y, Song R, Zheng T, Pan S, Pei T, et al. KIFC1 regulated by miR-532-3p promotes epithelial-to-mesenchymal transition and metastasis of hepatocellular carcinoma via gankyrin/AKT signaling. Oncogene. 2019;38:406–20.
17. Wang X, Wang M, Li XY, Li J, Zhao DP. KIFC1 promotes the proliferation of hepatocellular carcinoma in vitro and in vivo. Oncol Lett. 2019;18:5739–46.
18. Venere M, Horbinski C, Crish JF, Jin X, Vasanji A, Major J, Burrows AC, Chang C, Prokop J, Wu Q, et al. The mitotic kinesin KIF11 is a driver of invasion, proliferation, and self-renewal in glioblastoma. Sci Transl Med. 2015;7:304ra143.
19. Cho SY, Kim S, Kim G, Singh P, Kim DW. Integrative analysis of KIF4A, 9, 18A, and 23 and their clinical significance in low-grade glioma and glioblastoma. Sci Rep. 2019;9:4599.
20. Yamashita J, Fukushima S, Jinnin M, Honda N, Makino K, Sakai K, Masuguchi S, Inoue Y, Ihn H. Kinesin family member 20A is a novel melanoma-associated antigen. Acta Derm Venereol. 2012;92:593–7.
21. Jungwirth G, Yu T, Moustafa M, Rapp C, Warta R, Jungk C, Sahm F, Dettling S, Zweckberger K, Lamszus K, et al: **Identification of KIF11 As a Novel Target in Meningioma**. *Cancers (Basel)* 2019, **11**.
22. Zhang L, Zhu G, Wang X, Liao X, Huang R, Huang C, Huang P, Zhang J, Wang P. Genomewide investigation of the clinical significance and prospective molecular mechanisms of kinesin family member genes in patients with lung adenocarcinoma. Oncol Rep. 2019;42:1017–34.
23. Zhou K, Zhao J, Qi L, He Y, Xu J, Dai M. Kinesin Family Member C1 (KIFC1) Accelerates Proliferation and Invasion of Endometrial Cancer Cells Through Modulating the PI3K/AKT Signaling Pathway. Technol Cancer Res Treat. 2020;19:1533033820964217.
24. An L, Zhang J, Feng D, Zhao Y, Ouyang W, Shi R, Zhou X, Yu Z, Wei S, Min J, Wang H. KIF2C Is a Novel Prognostic Biomarker and Correlated with Immune Infiltration in Endometrial Cancer. Stem Cells Int. 2021;2021:1434856.
25. Podhorecka M, Skladanowski A, Bozko P: **H2AX Phosphorylation**: **Its Role in DNA Damage Response and Cancer Therapy**. *J Nucleic Acids* 2010, **2010**.
26. Bakkenist CJ, Kastan MB. DNA damage activates ATM through intermolecular autophosphorylation and dimer dissociation. Nature. 2003;421:499–506.
27. Banerjee D, Langberg K, Abbas S, Odermatt E, Yerramothu P, Volaric M, Reidenbach MA, Krentz KJ, Rubinstein CD, Brautigan DL, et al: **A non-canonical, interferon-independent signaling activity of cGAMP triggers DNA damage response signaling**. Nature Communications 2021, 12.

28. Walczak CE, Cai S, Khodjakov A. Mechanisms of chromosome behaviour during mitosis. Nat Rev Mol Cell Biol. 2010;11:91–102.
29. Zhu S, Paydar M, Wang F, Li Y, Wang L, Barrette B, Bessho T, Kwok BH, Peng A. **Kinesin Kif2C in regulation of DNA double strand break dynamics and repair**. Elife 2020, 9.
30. Luessing J, Sakhteh M, Sarai N, Frizzell L, Tsanov N, Ramberg KO, Maretto S, Crowley PB, Lowndes NF. The nuclear kinesin KIF18B promotes 53BP1-mediated DNA double-strand break repair. Cell Rep. 2021;35:109306.
31. Zhang L, Sun Y, Fei M, Tan C, Wu J, Zheng J, Tang J, Sun W, Lv Z, Bao J, et al. Disruption of chaperone-mediated autophagy-dependent degradation of MEF2A by oxidative stress-induced lysosome destabilization. Autophagy. 2014;10:1015–35.
32. Wittmann T, Wilm M, Karsenti E, Vernos I. TPX2, A novel xenopus MAP involved in spindle pole organization. J Cell Biol. 2000;149:1405–18.
33. Byrum AK, Carvajal-Maldonado D, Mudge MC, Valle-Garcia D, Majid MC, Patel R, Sowa ME, Gygi SP, Harper JW, Shi Y, et al. Mitotic regulators TPX2 and Aurora A protect DNA forks during replication stress by counteracting 53BP1 function. J Cell Biol. 2019;218:422–32.
34. Clarke MA, Devesa SS, Harvey SV, Wentzensen N. Hysterectomy-Corrected Uterine Corpus Cancer Incidence Trends and Differences in Relative Survival Reveal Racial Disparities and Rising Rates of Nonendometrioid Cancers. J Clin Oncol. 2019;37:1895–908.
35. Cote ML, Ruterbusch JJ, Olson SH, Lu K, Ali-Fehmi R. The Growing Burden of Endometrial Cancer: A Major Racial Disparity Affecting Black Women. Cancer Epidemiol Biomarkers Prev. 2015;24:1407–15.
36. Hou PF, Jiang T, Chen F, Shi PC, Li HQ, Bai J, Song J. KIF4A facilitates cell proliferation via induction of p21-mediated cell cycle progression and promotes metastasis in colorectal cancer. Cell Death Dis. 2018;9:477.
37. Huang Y, Wang H, Lian Y, Wu X, Zhou L, Wang J, Deng M, Huang Y. Upregulation of kinesin family member 4A enhanced cell proliferation via activation of Akt signaling and predicted a poor prognosis in hepatocellular carcinoma. Cell Death Dis. 2018;9:141.
38. Cho SY, Kim S, Kim G, Singh P, Kim DW. **Integrative analysis of KIF4A, 9, 18A, and 23 and their clinical significance in low-grade glioma and glioblastoma**. Scientific Reports 2019, 9.
39. Hu G, Yan Z, Zhang C, Cheng M, Yan Y, Wang Y, Deng L, Lu Q, Luo S. **FOXM1 promotes hepatocellular carcinoma progression by regulating KIF4A expression**. Journal of Experimental & Clinical Cancer Research 2019, 38.
40. Jungwirth Yu, Moustafa, Rapp, Warta, Jungk, Sahm, Dettling, Zweckberger, Lamszus, et al: **Identification of KIF11 As a Novel Target in Meningioma**. *Cancers* 2019, **11**.
41. Alhmoud JF, Woolley JF, Al Moustafa A-E, Malki MI. **DNA Damage/Repair Management in Cancers**. Cancers 2020, 12.
42. Alhmoud JF, Woolley JF, Al Moustafa AE, Malki MI. **DNA Damage/Repair Management in Cancers**. Cancers (Basel) 2020, 12.

43. Smith J, Tho LM, Xu N, Gillespie DA. The ATM-Chk2 and ATR-Chk1 pathways in DNA damage signaling and cancer. Adv Cancer Res. 2010;108:73–112.
44. Bartek J, Lukas J, Bartkova J. DNA damage response as an anti-cancer barrier: damage threshold and the concept of 'conditional haploinsufficiency'. Cell Cycle. 2007;6:2344–7.
45. Jaspers JE, Kersbergen A, Boon U, Sol W, van Deemter L, Zander SA, Drost R, Wientjens E, Ji J, Aly A, et al. Loss of 53BP1 causes PARP inhibitor resistance in Brca1-mutated mouse mammary tumors. Cancer Discov. 2013;3:68–81.
46. Wang J, Zhu C, Song D, Xia R, Yu W, Dang Y, Fei Y, Yu L, Wu J. Epigallocatechin-3-gallate enhances ER stress-induced cancer cell apoptosis by directly targeting PARP16 activity. Cell Death Discov. 2017;3:17034.
47. Bian X, Gao J, Luo F, Rui C, Zheng T, Wang D, Wang Y, Roberts TM, Liu P, Zhao JJ, Cheng H. PTEN deficiency sensitizes endometrioid endometrial cancer to compound PARP-PI3K inhibition but not PARP inhibition as monotherapy. Oncogene. 2018;37:341–51.
48. Bastos RN, Cundell MJ, Barr FA. KIF4A and PP2A-B56 form a spatially restricted feedback loop opposing Aurora B at the anaphase central spindle. J Cell Biol. 2014;207:683–93.
49. Hu CK, Coughlin M, Field CM, Mitchison TJ. KIF4 regulates midzone length during cytokinesis. Curr Biol. 2011;21:815–24.
50. Wu G, Zhou L, Khidr L, Guo XE, Kim W, Lee YM, Krasieva T, Chen PL. A novel role of the chromokinesin Kif4A in DNA damage response. Cell Cycle. 2008;7:2013–20.
51. Wan Q, Shen Y, Zhao H, Wang B, Zhao L, Zhang Y, Bu X, Wan M, Shen C. Impaired DNA double-strand breaks repair by kinesin family member 4A inhibition renders human H1299 non-small-cell lung cancer cells sensitive to cisplatin. J Cell Physiol. 2019;234:10360–71.
52. Hsu PK, Chen HY, Yeh YC, Yen CC, Wu YC, Hsu CP, Hsu WH, Chou TY. TPX2 expression is associated with cell proliferation and patient outcome in esophageal squamous cell carcinoma. J Gastroenterol. 2014;49:1231–40.
53. Tomii C, Inokuchi M, Takagi Y, Ishikawa T, Otsuki S, Uetake H, Kojima K, Kawano T. TPX2 expression is associated with poor survival in gastric cancer. World J Surg Oncol. 2017;15:14.
54. Sillars-Hardebol AH, Carvalho B, Tijssen M, Belien JA, de Wit M, Delis-van Diemen PM, Ponten F, van de Wiel MA, Fijneman RJ, Meijer GA. TPX2 and AURKA promote 20q amplicon-driven colorectal adenoma to carcinoma progression. Gut. 2012;61:1568–75.
55. Wang H, Wang X, Xu L, Cao H, Zhang J. **Nonnegative matrix factorization-based bioinformatics analysis reveals that TPX2 and SELENBP1 are two predictors of the inner sub-consensuses of lung adenocarcinoma**. Cancer Med 2021.
56. Neumayer G, Belzil C, Gruss OJ, Nguyen MD. TPX2: of spindle assembly, DNA damage response, and cancer. Cell Mol Life Sci. 2014;71:3027–47.
57. Bernassola F, Chillemi G, Melino G. HECT-Type E3 Ubiquitin Ligases in Cancer. Trends Biochem Sci. 2019;44:1057–75.

58. de Poot SAH, Tian G, Finley D. Meddling with Fate: The Proteasomal Deubiquitinating Enzymes. J Mol Biol. 2017;429:3525–45.
59. Lan H, Sun Y. Tumor Suppressor FBXW7 and Its Regulation of DNA Damage Response and Repair. Front Cell Dev Biol. 2021;9:751574.
60. Chen BR, Wang Y, Shen ZJ, Bennett A, Hindi I, Tyler JK, Sleckman BP. The RNF8 and RNF168 Ubiquitin Ligases Regulate Pro- and Anti-Resection Activities at Broken DNA Ends During Non-Homologous End Joining. DNA Repair (Amst). 2021;108:103217.
61. Moses N, Zhang M, Wu JY, Hu C, Xiang S, Geng X, Chen Y, Bai W, Zhang YW, Bepler G, Zhang XM. **HDAC6 Regulates Radiosensitivity of Non-Small Cell Lung Cancer by Promoting Degradation of Chk1**. Cells 2020, 9.
62. Cassidy KB, Bang S, Kurokawa M, Gerber SA. Direct regulation of Chk1 protein stability by E3 ubiquitin ligase HUWE1. FEBS J. 2020;287:1985–99.
63. Sharma N, Zhu Q, Wani G, He J, Wang QE, Wani AA. USP3 counteracts RNF168 via deubiquitinating H2A and gammaH2AX at lysine 13 and 15. Cell Cycle. 2014;13:106–14.
64. Yu H, Pak H, Hammond-Martel I, Ghram M, Rodrigue A, Daou S, Barbour H, Corbeil L, Hebert J, Drobetsky E, et al. Tumor suppressor and deubiquitinase BAP1 promotes DNA double-strand break repair. Proc Natl Acad Sci U S A. 2014;111:285–90.
65. Typas D, Luijsterburg MS, Wiegant WW, Diakatou M, Helfricht A, Thijssen PE, van den Broek B, Mullenders LH, van Attikum H. The de-ubiquitylating enzymes USP26 and USP37 regulate homologous recombination by counteracting RAP80. Nucleic Acids Res. 2016;44:2976.
66. Zhang H. **Regulation of DNA Replication Licensing and Re-Replication by Cdt1**. Int J Mol Sci 2021, 22.
67. Li Y, Yuan J. Role of deubiquitinating enzymes in DNA double-strand break repair. J Zhejiang Univ Sci B. 2021;22:63–72.

Tables

Table 1. Correlation between KIFA4A mRNA expression and clinicopathological

parameters of UCEC patients.

Parameter	KIF4A mRNA expression		*P*-value
	High(N=274)	Low(N=274)	
Age			
Mean (SD)	64.7 (10.7)	63.4 (11.4)	0.158
Median [Min, Max]	65.0 [33.0, 90.0]	63.0 [31.0, 90.0]	
FIGO Stage			
Stage	148 (54.0%)	194 (70.8%)	<0.001
Stage	31 (11.3%)	20 (7.3%)	
Stage	78 (28.5%)	48 (17.5%)	
Stage	17 (6.2%)	12 (4.4%)	
Histologic Grade			
G1	15 (5.5%)	83 (30.3%)	<0.001
G2	38 (13.9%)	82 (29.9%)	
G3	215 (78.5%)	104 (38.0%)	
Vital Status			
Alive	217 (79.2%)	238 (86.9%)	0.0228
Dead	57 (20.8%)	36 (13.1%)	
Histological Type			
EEA	178 (65.0%)	231 (84.3%)	<0.001
Mixed EA	15 (5.5%)	8 (2.9%)	
SEA	81 (29.6%)	35 (12.8%)	

EEA: Endometrioid endometrial adenocarcinoma; mixed EA: Mixed serous and endometrioid; SEA: Serous endometrial adenocarcinoma.

Figures

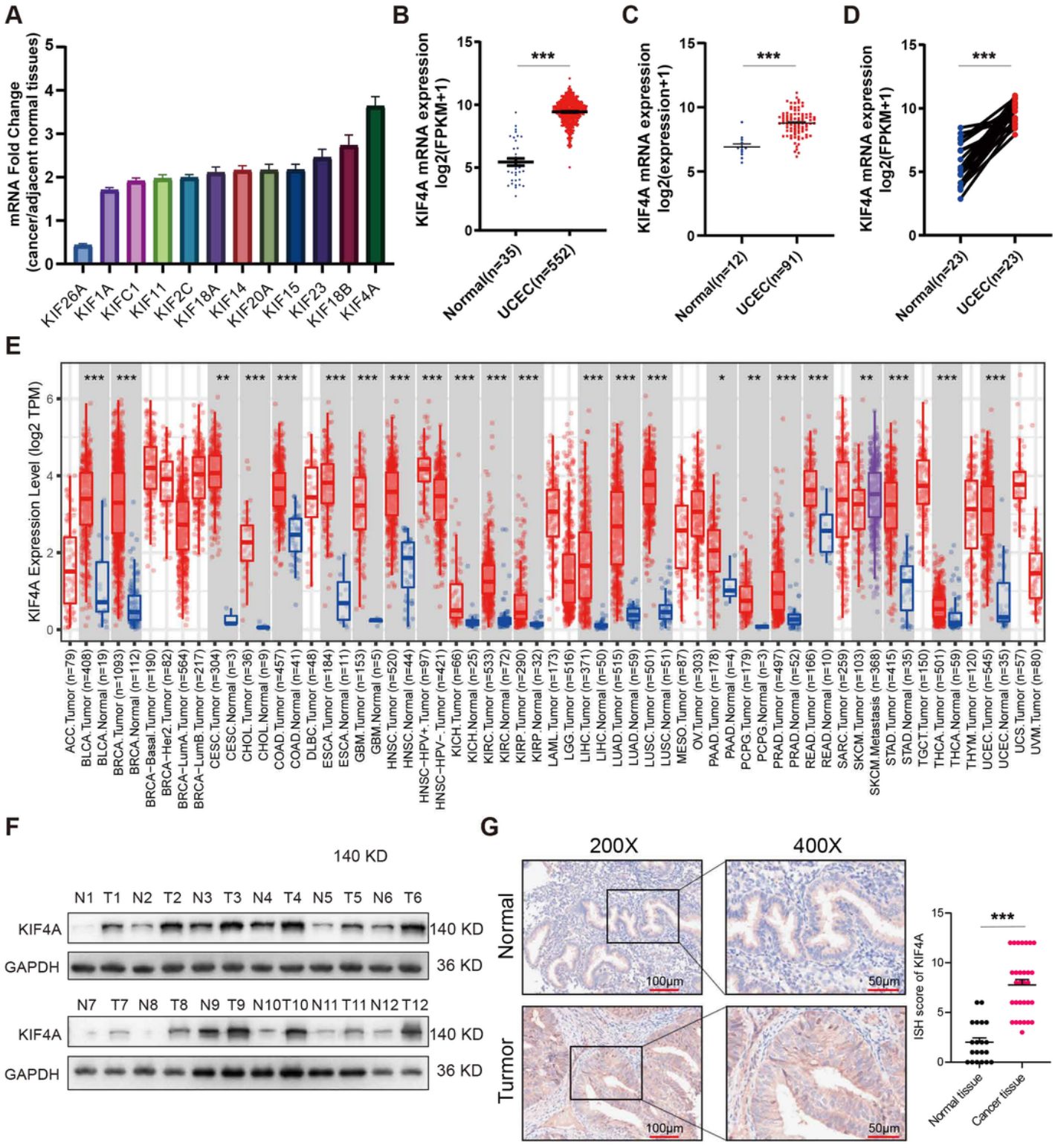

Figure 1

KIF4A was significantly upregulated in endometrial cancer in comparison with that of normal tissue.

(A) Fold change of the differentially expressed kinesins in endometrial cancer compared to that of adjacent normal tissues. (B) The mRNA levels of KIF4A in 552 UCEC tissues and 35 normal tissues in the TCGA database. *t-test*, ***$P < 0.001$. (C) The mRNA levels of KIF4A in 91 UCEC tissues and 12 normal

tissues in the GSE17025 database. *t-test*, ***P* < 0.001. (D) The mRNA levels of KIF4A in t23 paired samples from the TCGA database. *Paired t-test*, ***P* < 0.001. (E) The mRNA level of KIF4A in pan-cancer; data was derived from TIMER (http://timer.cistrome.org/). (F) The protein levels of KIF4A in UCEC tissues and adjacent normal tissues (Abbreviation: N, Normal tissue; T, Tumor tissue). (G) The immunohistochemistry (IHC) staining for KIF4A in UCEC tissues and adjacent normal tissues. *t-test*, **P* < 0.01. 20X, scale bars = 100 μm; 40X, scale bars = 50 μm.

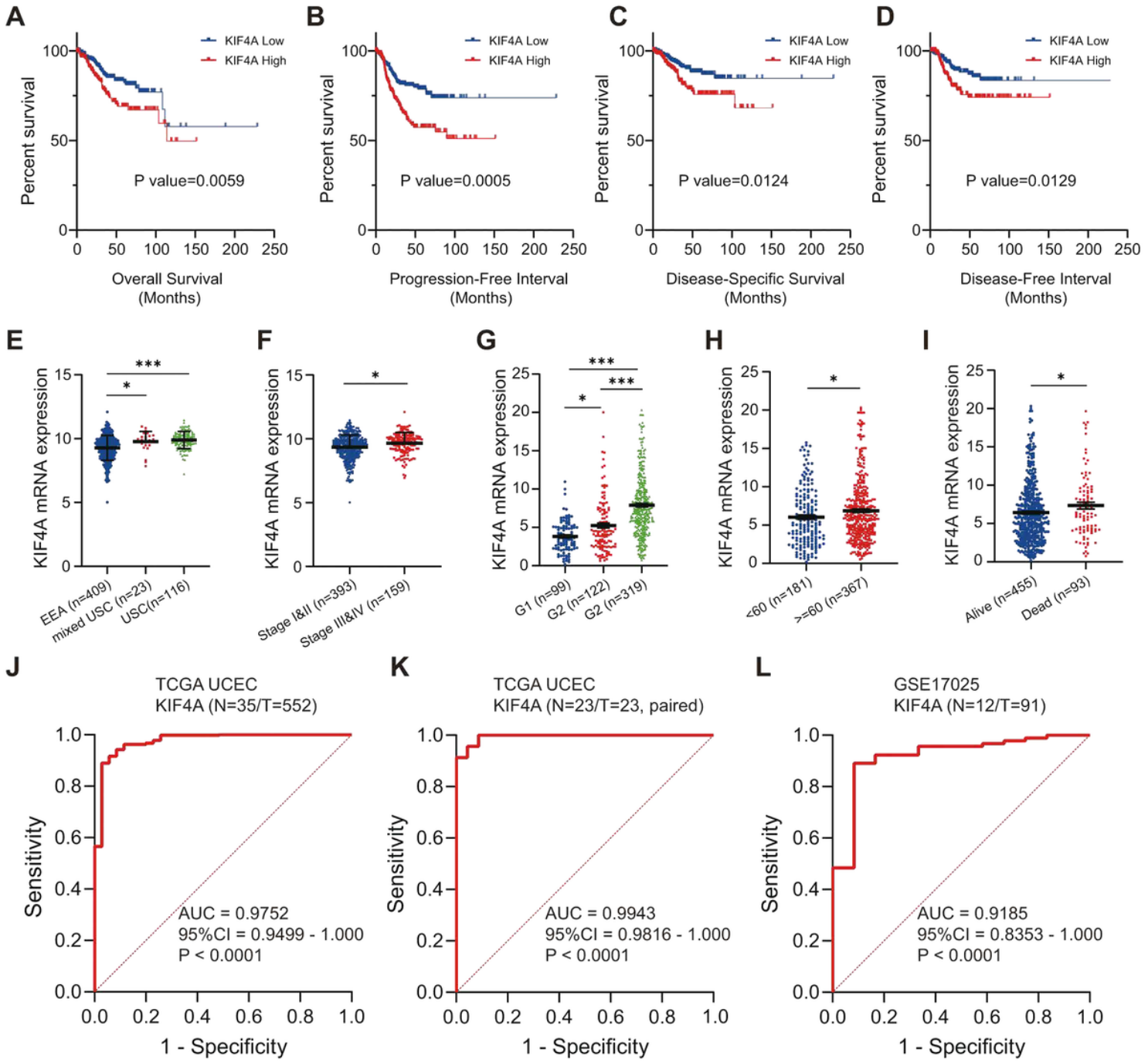

Figure 2

KIF4A predicted poor prognosis in UCEC and was correlated with clinicopathological features.

(A-D) The Kaplan–Meier curves of KIF4A in UCEC for both Overall Survival (OS), Progression-Free Interval (PFI), Disease-Specific Survival (DSS), and Disease-Free Interval (DFI). (E-I) The mRNA level of KIF4A in TCGA UCEC patients among different subgroups including pathology type, clinical stage, histologic grade, age, and vital status. *t-test* and *One way-ANOVA*.***, *P* <0.001, **, *P* <0.01, *, *P* <0.05, *P* = ns (no significance). (J-K) The ROC (receiver operating characteristic) curves of KIF4A in TCGA UCEC (AUC : 0.9752, 95%CI : 0.9499 - 1.000, *P* < 0.0001), TCGA paired samples (AUC: 0.9943, 95%CI: 0.9816 - 1.000, *P* < 0.0001), and GSE17025 (AUC = 0.9185, 95%CI: 0.8353 - 1.000, *P* < 0.0001) datasets.

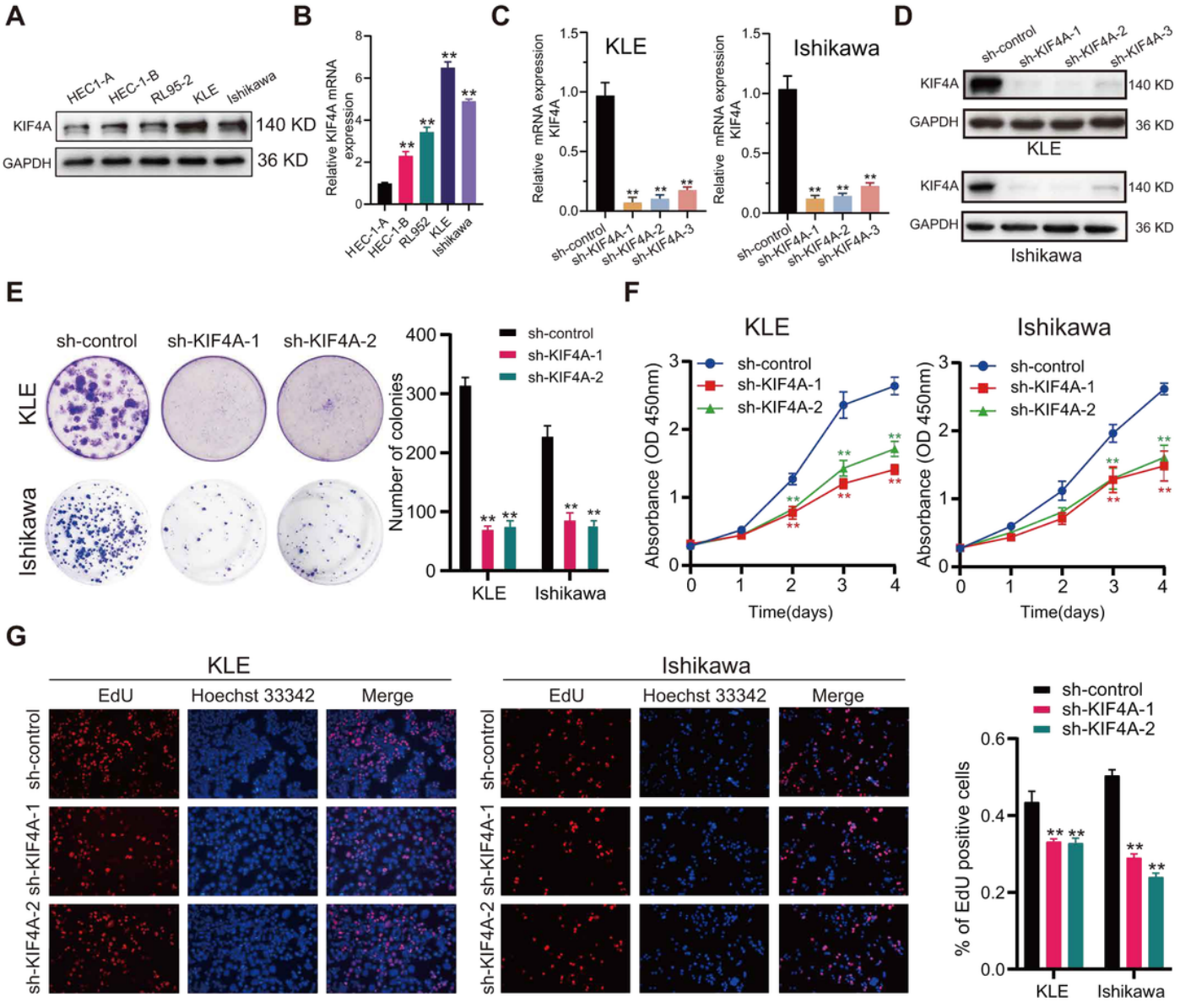

Figure 3

KIF4A knockdown suppresses proliferation of endometrial cancer cells in vitro

(A-B) The protein and mRNA levels in five EC cell lines (HEC1-A, HEC-1-B, RL95-2, KLE, and Ishikawa). (C-D) The efficient knockdown of KIF4A by shRNAs was verified by quantitative reverse transcription PCR (qRT-PCR) analysis or western blotting. (E) Representative putative clone formation of EC cells with KIF4A

knockdown or empty vector control at 2 weeks. (F) CCK8 assay was performed to observe inhibition effects of KIF4A knockdown. (G) EdU staining of KLE and Ishikawa cells, and the quantifications of EdU-positive cell proportion.

t-test .***$P < 0.001$, **$P < 0.01$.

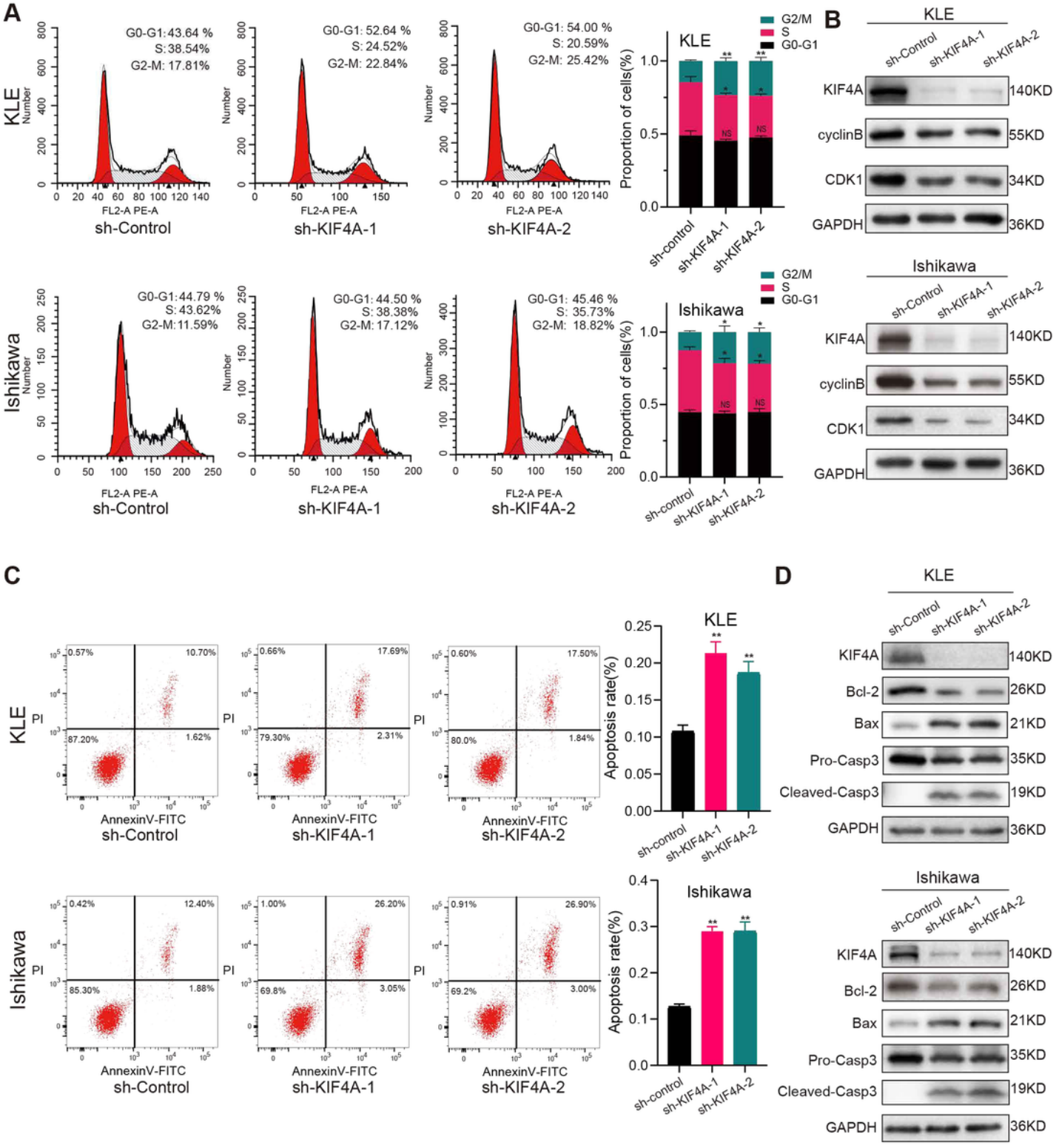

Figure 4

Knockdown of KIF4A induces cell cycle arrest and apoptosis

(A) Flow cytometric cell cycle analysis of PI-stained EC cells with or without KIF4A knockdown. (B) Western blot analyses with cyclinB1 and CDK1 antibodies of KIF4A knockdown and negative control EC cells. (C) Apoptosis was measured by flow cytometry using PI/Annexin V staining. (D). The effects of KIF4A knockdown on the expression of apoptosis-related proteins (BAX, cleaved Caspase3, and BCL2) were examined by western blot analysis. Data are presented as mean ± SEM. *** $P < 0.001$, ** $P < 0.01$,* $P < 0.05$.

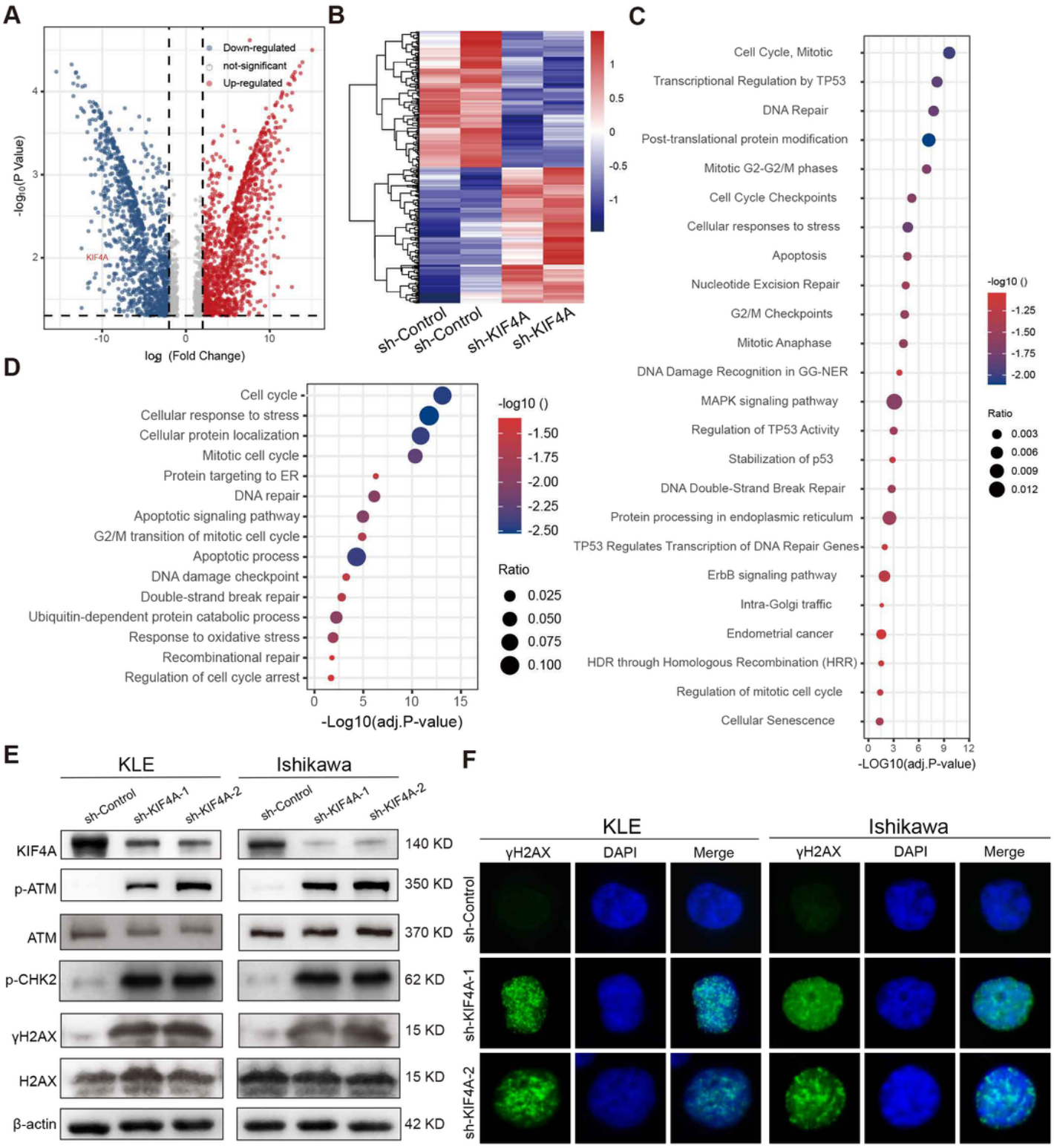

Figure 5

KIF4A knockdown cells accumulate DNA lesions that activate DNA damage responses

(A-B) Volcano plot and heatmap depict differentially expressed genes between KIF4A knockdown and control transduced KLE cells. (C-D) Pathway enrichment analysis and GO enrichment analysis of differentially expressed genes. (E) Western blot showing the phosphorylation status of DDR signaling

proteins H2AX (γH2AX), ATM (pATM), and pCHK2 in KLE and Ishikawa cells with or without KIF4A knockdown. (F) Immunofluorescence staining of γH2AX foci in EC cells.

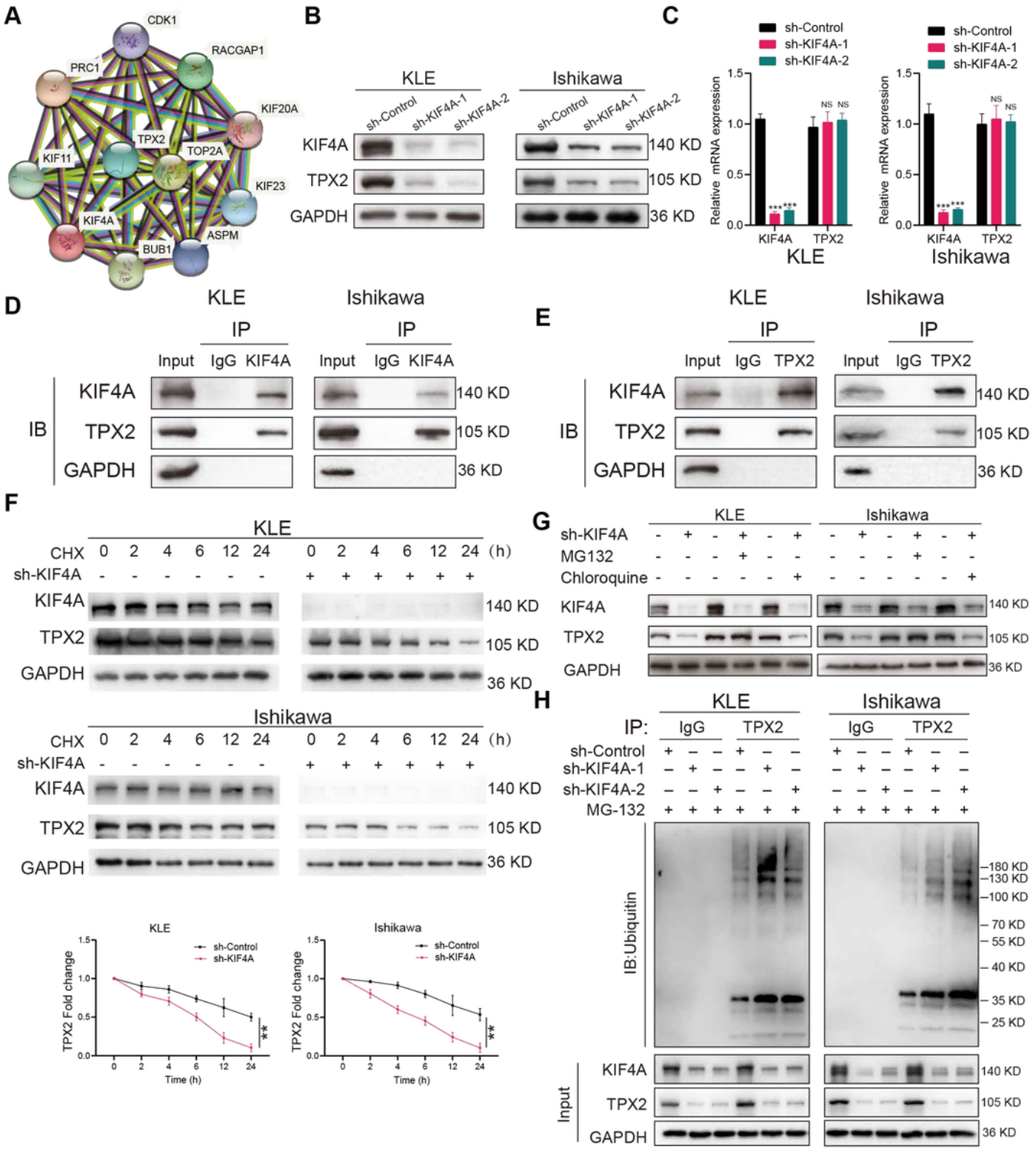

Figure 6

KIF4A regulated the protein stability of TPX2

(A) Top 10 KIF4A-interacting proteins were identified from the STRING database (http://string-db.org). (B-C) Western blot and qPCR were performed to examine the protein and mRNA levels of TPX2 following KIF4A knockdown in KLE and Ishikawa cells. (D-E) The interaction between endogenous KIF4A and TPX2 was determined by CO-IP and western blotting. (F) EC cells with stable KIF4A knockdown were treated with cycloheximide (CHX, 10 μmol/L) to inhibit protein synthesis for the indicated times, and TPX2 protein turnover was analyzed over time. One representative experiment of 3 independent experiments is shown. (G) EC cells with stable KIF4A knockdown were treated with DMSO, MG132 (20 μM), or chloroquine (50 μM) for 12 h. Western blotting was used to examine the protein level of TPX2. (H) The EC cells with stable KIF4A knockdown were lysed and subjected to immunoprecipitation with an antibody against TPX2 and analyzed by western blotting with an anti-ubiquitin antibody.

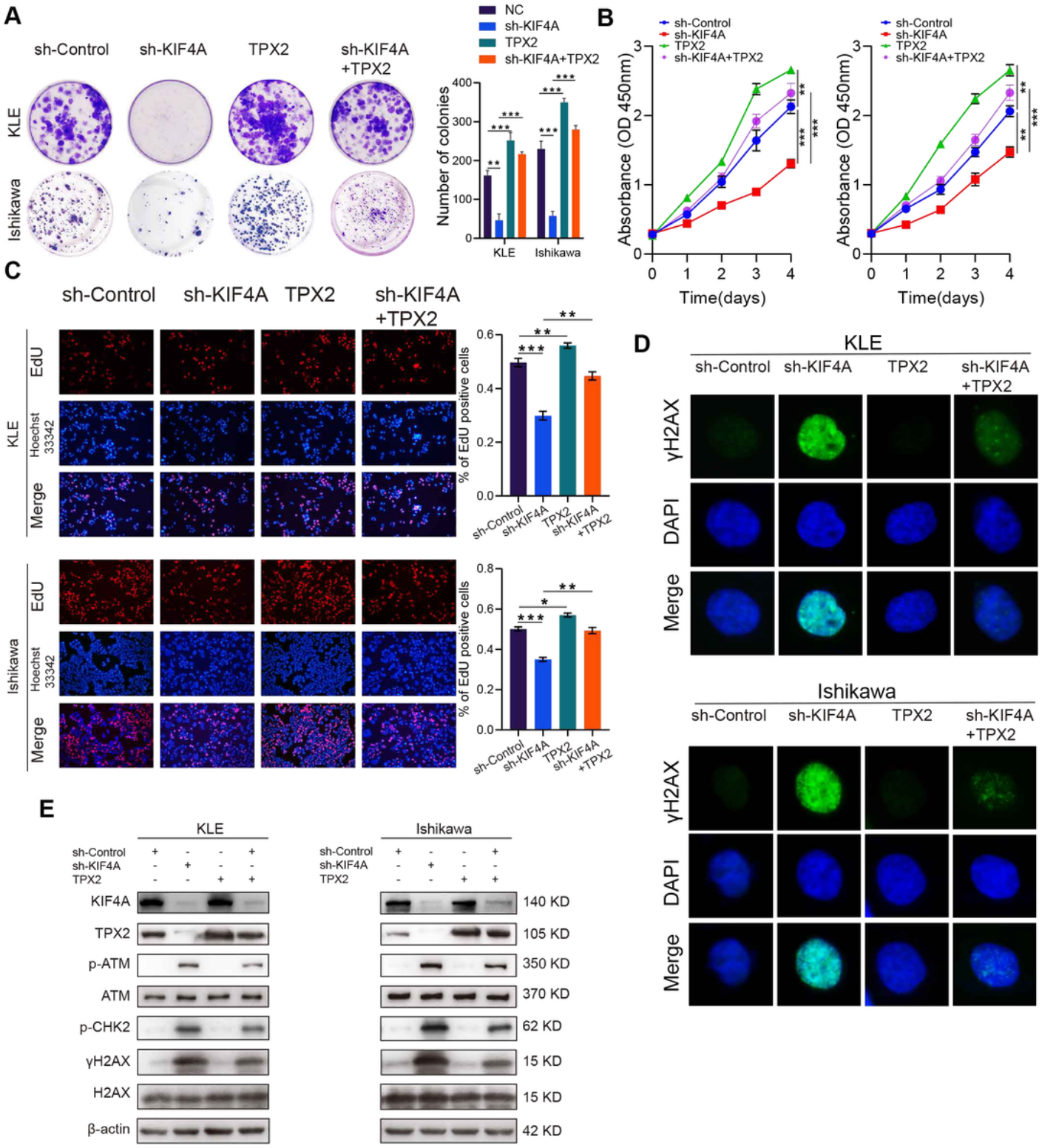

Figure 7

TPX2 was required for KIF4A-mediated tumor progression

(A) Colony formation assay and (B) CCK-8 assay demonstrated that TPX2 overexpression abolished the decreased growth abilities of EC cells caused by KIF4A knockdown. *t-test*, *** $P < 0.001$; ** $P < 0.01$; * $P < 0.05$. (C) EdU assay showed that TPX2 overexpression could rescue the decreased EdU-positive rates of

EC cells induced by KIF4A knockdown. *t-test*, *** $P < 0.001$; ** $P < 0.01$; * $P < 0.05$. (D) KLE and Ishikawa cells were infected with the indicated lentivirus or plasmids. Cells were then fixed for immunofluorescent staining of γH2AX. (E) Western blotting analysis showed that TPX2 overexpression abolished the increased DDR signaling.

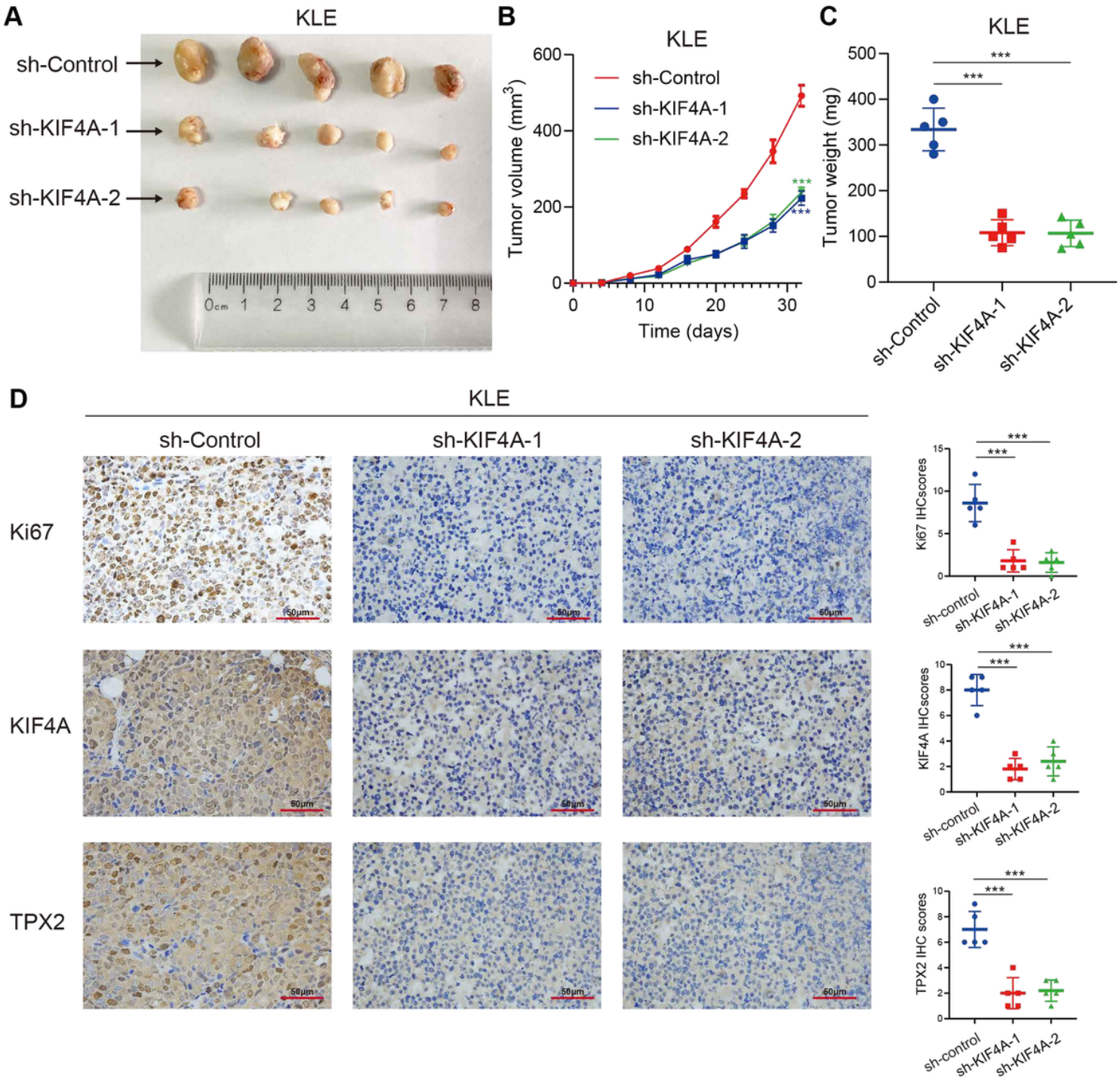

Figure 8

KIF4A knockdown inhibited xenograft tumor growth

(A) The nude mice bearing KLE xenografts with stable KIF4A knockdown were treated with vector control. (B) Xenograft tumor volumes were measured every 4 d when they were palpable. (C) The tumor weight of the xenografts after dissection. (D) Representative photographs of IHC staining of ki-67, KIF4A, and TPX2 in xenograft tumors, and the statistical results of the IHC scores, respectively. t-test; ***$P < 0.001$; **$P < 0.01$; *$P < 0.05$.

Supplementary Files

This is a list of supplementary files associated with this preprint. Click to download.

- SupplementaryMaterial.docx